Thickness Control of Colloidal Crystals with a Substrate Dipped at a Tilted Angle into a Colloidal Suspension

Sang Hyuk Im, Mun Ho Kim, and O Ok Park*

Department of Chemical and Biomolecular Engineering, Korea Advanced Institute of Science and Technology, 373-1 Guseong-dong, Yuseong-gu, Daejeon, 305-701, Republic of Korea

Received December 16, 2002. Revised Manuscript Received February 28, 2003

When a glass substrate is dipped into a colloidal suspension, the contact line shape is changed with the angle of tilt. These variations in the contact line shape indicate a possibility for thickness control of colloidal crystals. Thus, we have investigated how the thickness of colloidal crystals is changed with specific tilted angles (−10°, 0°, 10°, 20°, and 30°, respectively). As a glass substrate is tilted more (from −10° to 30°), a smoother and thicker contact line is formed and thicker colloidal crystals are obtained. In addition, it is possible to explain why multiple contact line patterns are formed on the glass substrate. It was found that to fabricate three-dimensional colloidal crystals with an even surface, the evaporation rate of water should be reduced and/or the glass substrate should be tilted over 10° in our cases.

Introduction

Three-dimensional (3D) photonic band gap (PBG) crystals of the order of an optical wavelength have attracted a great deal of attention because of their ability to manipulate, confine, and control light.[1−3] These crystals have potential use in various applications such as waveguides,[4] optical filters,[5] switches,[6] high-density magnetic data storage devices,[7] and chemical and biochemical sensors.[8] Accordingly, intensive studies have been performed over the last few decades to fabricate 3D regular structures. Several strategies have been exploited for the creation of 3D PBG structures, including the chemical methods of colloidal self-assembly[9−12] and colloidal crystal templating,[13−21] the microfabrication techniques of mechanically drilling holes within a dielectric slab or stacking logs of a dielectric or metallic materials,[22−24] and holographic patterning using multiple laser beams.[25−27] Among these approaches, the fabrication of 3D PBG crystals via colloidal self-assembly is particularly attractive. In addition to being inexpensive, this method offers relative ease of processing and requires short processing time, compared to the stepwise manner of microfabrication techniques. Typical methods for colloidal self-assembly are gravitational sedimentation of colloidal particles,[28] vertical deposition,[29−31] vertical deposition with temperature

* To whom correspondence should be addressed. E-mail: oopark@kaist.ac.kr.

(1) Joannopoulos, J. D.; Meade, R. D.; Winn, J. N. *Photonic Crystals: Molding the Flow of Light*; Princeton University Press: Princeton, NJ, 1995.
(2) Yablonovitch, E. *Phys. Rev. Lett.* **1987**, *58*, 2059−2062.
(3) John, S. *Phys, Rev. Lett.* **1987**, *58*, 2486−2489.
(4) Vogelaar, L.; Nijda, W.; van Wolferen, H. A. G. M.; de Ridder, R. M.; Segerink, F. B.; Kuipers, E. F. L.; van Hulst, N. F. *Adv. Mater.* **2001**, *13*, 1551−1554.
(5) Park, S. H.; Xia, Y. *Langmuir* **1999**, *15*, 266−273.
(6) Tran, P. *J. Opt. Soc. Am. B* **1997**, *14*, 2589−2595.
(7) Cumpston, B. H.; Ananthavel, S. P.; Barlow, S.; Dyer, D. L.; Ehrlich, J. E.; Erskine, L. L.; Heikal, A. A.; Kuebler, S. M.; Lee. I. Y. S.; McCord-Maughon D.; Qin, j. Q.; Rockel, H.; Rumi, M.; Wu, X. L.; Marder, S. R.; Perry, J. W. *Nature* **1999**, *398*, 51−54.
(8) Lee, K.; Asher, S. A. *J. Am. Chem. Soc.* **2000**, *122*, 9534−9537.
(9) Romanov, S. G.; Johnson, N. P.; Fokin, A. V.; Butko, V. Y.; Yates, H. M.; Pemble, M. E.; Sotomayor Torres, C. M. *Appl. Phys. Lett.* **1997**, *70*, 2091−2093.
(10) Mayoral, R.; Requena, J.; Moya, J. S.; Lopez, C.; Cintas, A.; Miguez, H.; Meseguer, F.; Vazquez, L.; Holgado, M.; Blanco, A. *Adv. Mater.* **1997**, *9*, 257−260.
(11) Egen, M.; Zentel, R. *Chem. Mater.* **2002**, *14*, 2176−2183.
(12) Schroden, R. C.; Mohmmed, A.-D.; Stein, A. *Chem. Mater.* **2001**, *13*, 2945−2950.
(13) Schroden, R. C.; Mohammed, A.-D.; Blanford, C. F.; Stein A. *Chem. Mater.* **2002**, *14*, 3305−3315.
(14) Holland, B. T.; Blanford, C. F.; Do, T.; Stein A. *Chem. Mater.* **1999**, *11*, 795−805.
(15) Wijnhoven, J. E. G. J.; Vos, W. L. *Science* **1998**, *281*, 802−804.
(16) Velev, O. D.; Tessier, P. M.; Lenhoff, A. M.; Kaler, E. W. *Nature* **1999**, *401*, 548.
(17) Braun, P. V.; Wiltzius, P. *Nature* **1999**, *402*, 603−604.
(18) Velev, O. D.; Kaler, E. W. *Adv. Mater.* **2000**, *12*, 531−534.
(19) Vlasov, Y. A.; Yao, N.; Norris, D. J. *Adv. Mater.* **1999**, *11*, 165−169.
(20) Yan. H.; Blanford, C. F.; Holland, B. T.; Smyrl, W. H.; Stein, A. *Chem. Mater.* **2000**, *12*, 1134−1141.
(21) Blanco, A.; Chomski, E.; Grabtchak, S.; Ibisate, M.; John, S.; Leonard, S. W.; Lopez, C.; Meseguer, F.; Miguez, H.; Mondia, J. P.; Ozin, G. A.; Toader, O.; van Driel, H. M. *Nature* **2000**, *405*, 437−440.
(22) Yablonovitch, E.; Gmitter, T. J.; Leung, K. M. *Phys. Rev. Lett.* **1991**, *67*, 2295−2298.
(23) Fleming, J. G.; Lin, S. Y.; El-Kady, I.; Biswas, R.; Ho, K. M. *Nature* **2002**, *417*, 52−55.
(24) Lin, S. Y.; Fleming, J. G.; Hetherington, D. L.; Smith, B. K.; Biswas, R.; Ho, K. M.; Sigalas, M. M.; Zubrzycki, W.; Kurtz, S. R.; Bur, J. *Nature* **1998**, *394*, 251−253.
(25) Campbell, M.; Sharp, D. N.; Harrison, M. T.; Denning, R. G.; Turberfield, A. J. *Nature* **2000**, *404*, 53−56.
(26) Sun, H.-B.; Matsuo, S.; Misawa, H. *Appl. Phys. Lett.* **1999**, *74*, 786−788.
(27) Yang, S.; Megens, M.; Aizenberg, J.; Wiltzius, P.; Chaikin, P. M.; Russel, W. B. *Chem. Mater.* **2002**, *14*, 2831−2833.
(28) Miguez, H.; Meseguer, F.; Lopez, C.; Blanco, A.; Moya, J.; Requena, J.; Mifsud, A.; Fornes, V. *Adv. Mater.* **1998**, *10*, 480−483.
(29) Jiang. P.; Bertone, J. F.; Hwang, K. S.; Colvin, V. L. *Chem. Mater.* **1999**, *11*, 2132−2140.
(30) Ye, Y. H.; LeBlanc, F.; Hache, A.; Truong, V. V. *Appl. Phys. Lett.* **2001**, *78*, 52−54.
(31) Goldenberg, L. M.; Wagner, J.; Stumpe, J.; Paulke, B.-R.; Gornitz, E. *Langmuir* **2002**, *18*, 3319−3323.

10.1021/cm021793m CCC: $25.00
Published on Web 04/04/2003

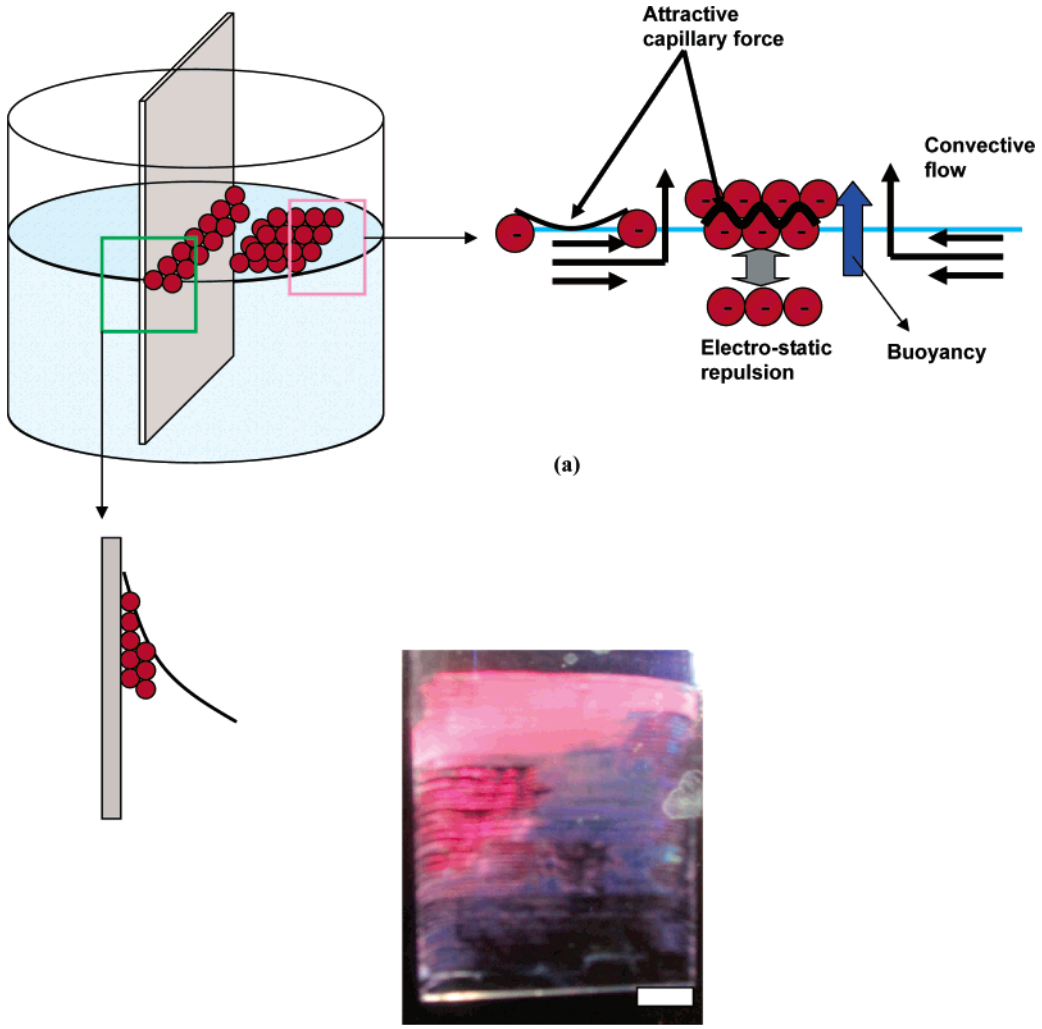

Figure 1. (a) Systematic illustration of 3D colloidal assembly at an air−water−glass substrate interface (green square) and an air−water interface[35] (pink square). (b) Photograph of −10° tilted sample (normal incident viewing). The upper part shaded in red is formed by assembled 3D colloidal crystals at the air−water interface and the lower part shown in blue is assembled at the air−water−glass substrate interface. The 0° sample shows a similar pattern. The scale bar is 5 mm.

gradient,[32] electrophoresis,[33] ice crystallization,[34] colloidal assembly at an air−water interface,[35] and colloidal assembly on a liquid metal surface.[36]

Thick colloidal PBG crystals are necessary for use in optical band stop filters because reflectance is a function of the number of stacked layers in colloidal crystals. As such, it is very important to control the thickness of colloidal crystals. Generally, crystal thickness has been controlled by the concentration of colloidal suspensions;[29] thicker colloidal crystals are obtained in higher concentrations of a suspension. In this paper, we report that the thickness of colloidal crystals can be controlled according to the tilted angle of a glass substrate dipped into a colloidal suspension with a fixed concentration. In addition, we have explained how colloidal particles deposit onto the dipped substrate.

Experimental Section

Polystyrene (PS) sub-micrometer-sized particles as building blocks of photonic crystals were synthesized by emulsifier-free emulsion polymerization.[37,38] Deionized water (450 g) was poured into a reactor and the water was kept at a temperature of 80 °C and stirred at 350 rpm. Sodium styrene sulfonate (0.25 g) as an emulsifier and sodium hydrogen carbonate (0.25 g) as a buffer were inserted into the water. After 10 min, styrene monomer (50 g) was inserted into the solution. After 1 h, potassium persulfate (0.25 g) was introduced as an initiator into the solution. Finally, polymerization was performed under a nitrogen atmosphere for 18 h.

The effective diameter of the prepared PS colloidal particles measured by dynamic light scattering (Zeta Plus, Brookhaven Instrument Corp.) was 265 nm, and their polydispersity was 0.005. The values are averages of five measurements. The diameter of the corresponding PS colloids measured by scanning electron microscopy (SEM) was 260 nm.

To assemble 3D colloidal crystals and to control the thickness of colloidal crystals, glass substrates without particular pretreatments excluding cleaning with ethanol were dipped

(32) Vlasov, Y. A.; Bo, X.-Z.; Sturm, J. C.; Norris, D. J. *Nature* **2001**, *414*, 289−293.
(33) Rogach, A. L.; Kotov, N. A.; Koktysh, D. S.; Ostrander, J. W.; Ragoisha, G. A. *Chem. Mater.* **2000**, *12*, 2721−2726.
(34) Im, S. H.; Park, O O. *Appl. Phys. Lett.* **2002**, *80*, 4133−4135.
(35) Im, S. H.; Lim, Y. T.; Suh, D. J.; Park, O O. *Adv. Mater.* **2002**, *14*, 1367−1369.
(36) Griesebock, B.; Egen, M.; Zentel, R. *Chem. Mater.* **2002**, *14*, 4023−4025.
(37) Yi, G. R.; Moon, J. H.; Yang, S.-M. *Chem. Mater.* **2001**, *13*, 2613−2618.
(38) Kim, J. H.; Chainey, M.; El-Aasser, M. S.; Vanderhoff, J. W. *J. Polym. Sci., Polym. Chem.* **1992**, *30*, 171−183.

into 0.2 wt % PS colloidal suspensions (40 mL) with specific tilted angles (−10°, 0°, 10°, 20°, and 30°, respectively). The colloidal suspensions were placed in a furnace of 60 °C and water was evaporated at a rate of 0.7 mL/h.

Results and Discussion

3D Colloidal Assembly. To fabricate 3D regular structures, water was evaporated from a 260-nm PS colloidal suspension (0.2 wt %) at a rate of 0.7 mL/h in a furnace of 60°C while dipping a glass substrate into the suspension. Under these conditions, a 3D colloidal assembly occurs at two different interfaces, as depicted in Figure 1a. An assembly is formed at the air−water interface[35] and another is generated at the air−water−glass substrate interface.[29−31] The reason for the formation of a 3D regular structure at the air−water interface is as follows: First, the PS colloidal particles protrude easily from the water surface by evaporation of water. Then, the strong attractive capillary force causes the colloidal particles to assemble into ordered regions. These ordered regions grow due to the convective transport of particles to the ordered region. When particles assemble toward ordered regions by convective flow, the effective density of the ordered arrays becomes lower than the density of water. Hence, the arrays float toward the water surface. Therefore, multiple layers are formed on the water surface by further evaporation of water.[35] The colloidal suspension is contained in a wettable vessel (Pyrex beaker; 50 mL, diameter = 4 cm) and thus the surface of the suspension becomes concave. Accordingly, the ordered microstructures on the water surface assemble at the center region because the evaporation rate of water is greatest at the center region. It is well-established that colloidal particles assemble two- or three-dimensionally in an air−water−glass substrate (any available wettable substrate). Nagayama's groups[39−43] have reported on 2D arrays and Colvin's groups[29,44] have investigated 3D arrays.

In the present study, the 3D ordered areas on the water surface are relatively small and thus the corresponding ordered arrays deposit onto a part of the glass substrate and ordered colloidal particles assembled at the air−water-glass substrate interface are deposited onto other parts of the glass substrate. Figure 1b shows the resulting morphology of a sample (−10° tilted substrate, see Figure 2a). The upper part appearing in red shows the ordered microstructures at the air−water interface; this clearly shows that the ordered areas on the water surface are small, and the lower part shows the ordered arrays at the air−water−glass substrate. This figure is evidence that 3D colloidal assembly occurs at two different interfaces. As expected, the occupying areas of the ordered microstructures on the water surface can be reduced by decreasing the water evaporation rate (controlling temperature and humidity) and colloidal suspension concentration. In the present study, we focus on how the thickness of colloidal crystals created only at the air−water−glass substrate interface changes with the tilted angle of a dipped glass substrate.

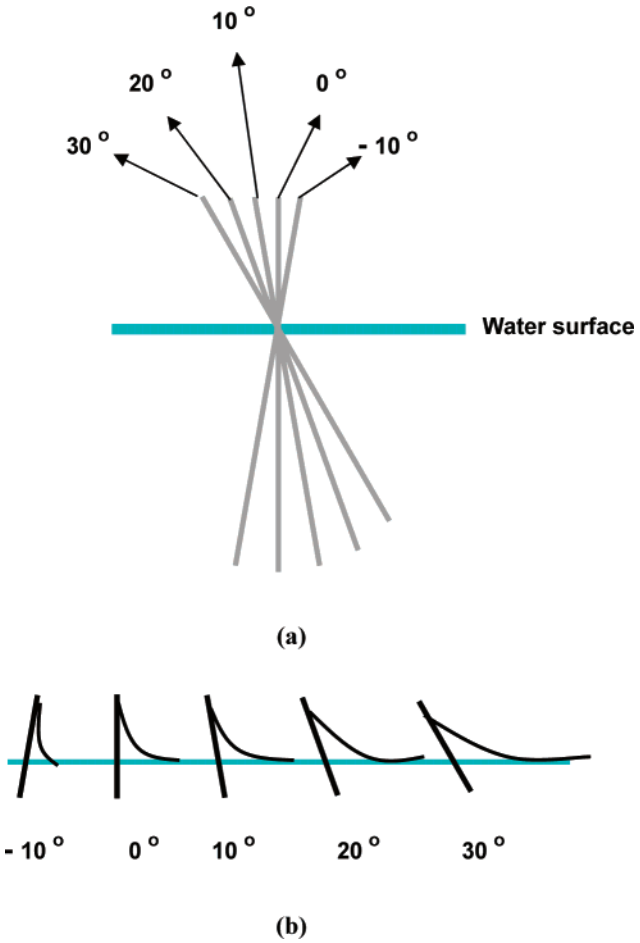

Figure 2. (a) We defined that the normal to the water surface plane is 0° and established tilted angles −10°, 0°, 10°, 20°, and 30°, respectively. (b) Contact line shapes with tilted angles.

Thickness Control of Colloidal Crystals. It is important to control the thickness of colloidal crystals because thickness is related to the crystals' optical properties (reflectance). Generally, reflectance of colloidal crystals (depth of the photonic band gap) increases as the number of stacked layers increases because the number of layers reflecting specific wavelength increases. However, it is not necessary for the colloidal crystals to have very large thicknesses because the intensity of light attenuates rapidly with propagation distance into the crystals and consequently increasing the thickness of the crystals above a certain critical thickness has little effect on the reflectance.[29,44]

To control the thickness of the colloidal crystals, we changed the contact line shape at the air−water−glass substrate by varying the tilted angle of a glass substrate dipped into the colloidal suspension, as shown in Figure 2a. The contact line shapes of each sample are depicted in Figure 2b. The contact line shape of the sample tilted to −10° is the steepest and gradually becomes smoother as the tilted angle increases. These contact line shapes imply that the thickness of ordered colloidal particles assembling in the vicinity of the air−water−glass substrate interface can be controlled by the tilted angle

(39) Denkov, N. D.; Velev, O. D.; Kralchevsky, P. A.; Ivanov, I. B.; Yoshimura, H.; Nagayama, K. *Nature* **1993**, *361*, 26.
(40) Denkov, N. D.; Velev, O. D.; Kralchevsky, P. A.; Ivanov, I. B.; Yoshimura, H.; Nagayama, K. *Langmuir* **1992**, *8*, 3183−3190.
(41) Adachi, E.; Dimitrov, A. S.; Nagayama, K. *Langmuir* **1995**, *11*, 1057−1060.
(42) Dimitrov, A. S.; Nagayama, K. *Langmuir* **1996**, *12*, 1303−1311.
(43) Yamaki, M.; Higo, J.; Nagayama, K. *Langmuir* **1995**, *11*, 2975−2978.
(44) Bertone, J. F.; Jiang, P.; Hwang, K. S.; Mittleman, D. M. Colvin, V. L. *Phys. Rev. Lett.* **1999**, *83*, 300−303, and references therein.

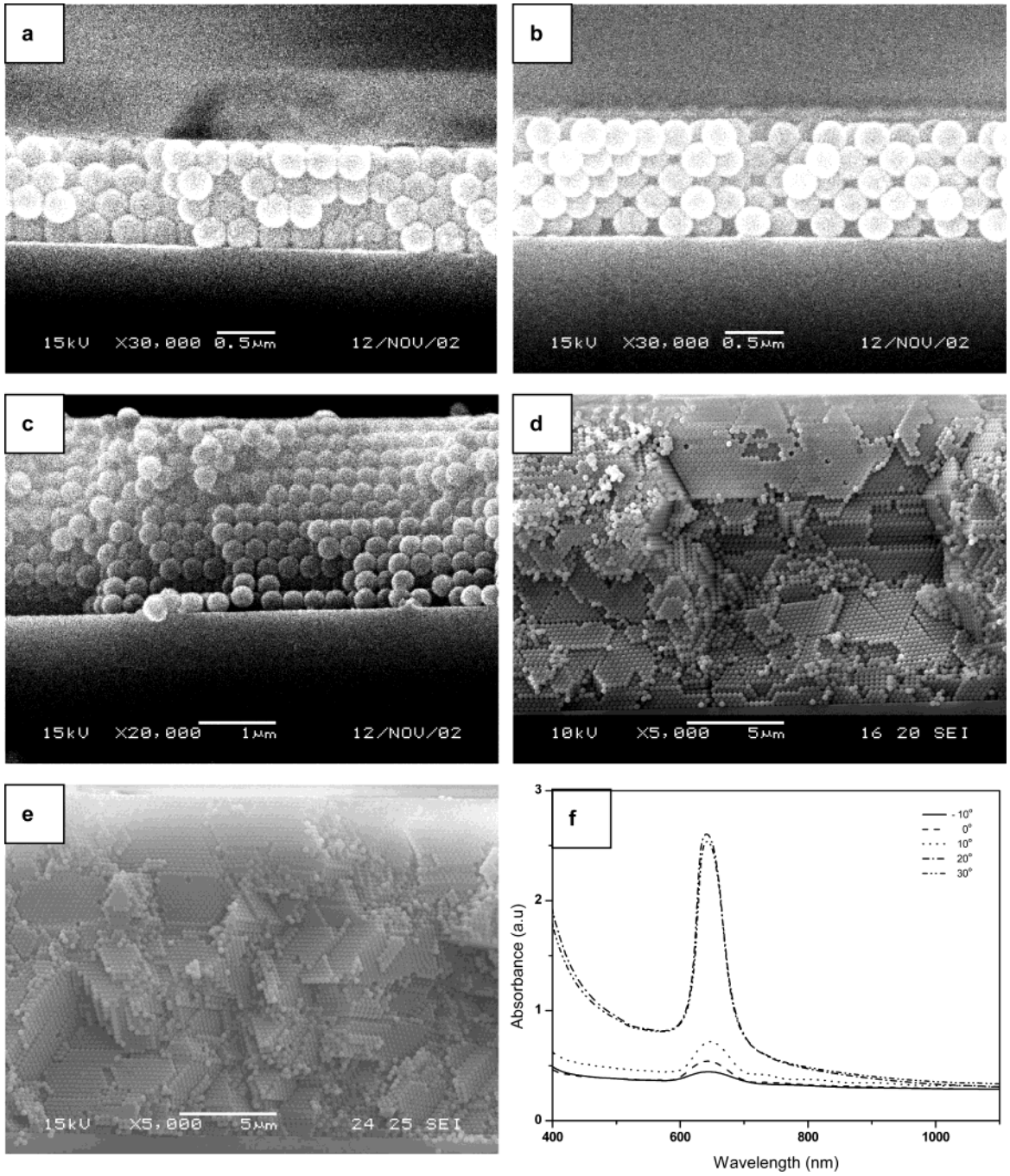

Figure 3. Cross-sectional SEM images: (a) −10°, (b) 0°, (c) 10°, (d) 20°, and (e) 30°. (f) UV−vis absorbance spectra.

of the dipped glass substrate. Cross-sectional SEM images of each sample are shown in Figure 3a−e. All images represent regions of assembled colloidal particles at the air−water−glass substrate interface. In Figure 2b, as anticipated, the thickness of the colloidal crystals increases as the tilted angle becomes higher. All samples show that the (111) planes of face-centered cubic (fcc) structures are oriented parallel to the substrate and colloidal crystals are highly ordered (see Figure (a) in the Supporting Information). The samples tilted to −10° and 0° have very steep contact line shapes, and thus the thickness of colloidal crystals that assemble at the interface becomes small. Samples tilted to 20° and 30° provide sufficient thickness for colloidal particles to assemble at the interface because the contact line shapes are smooth. For the same reason, the sample tilted to 10° has an intermediate thickness of the samples tilted to 0° and 20°. In addition, the samples tilted to −10° and 0° show wrinkled surfaces (multiple contact line patterns: thick layers (Figure 3b) and thin layers (Figures (b) and (c) in the Supporting Information) appear alternatively) as shown in Figure 1b, while the other samples show even surfaces as shown in Figure 4c. (Explanations for these observations are provided in the following section.) These observations indicate that it is necessary to dip the glass substrate into the colloidal suspension at an angle greater than 10° to obtain colloidal crystals with an even surface.

The transmission spectra of colloidal crystals can represent colloidal crystal states because the presence of defects in colloidal crystals affects the photonic band tail states and thus enhances the transmission in the gap.[30] We measured absorption spectra (Figure 3f) using ultraviolet−visible (UV−vis) spectroscopy because PS

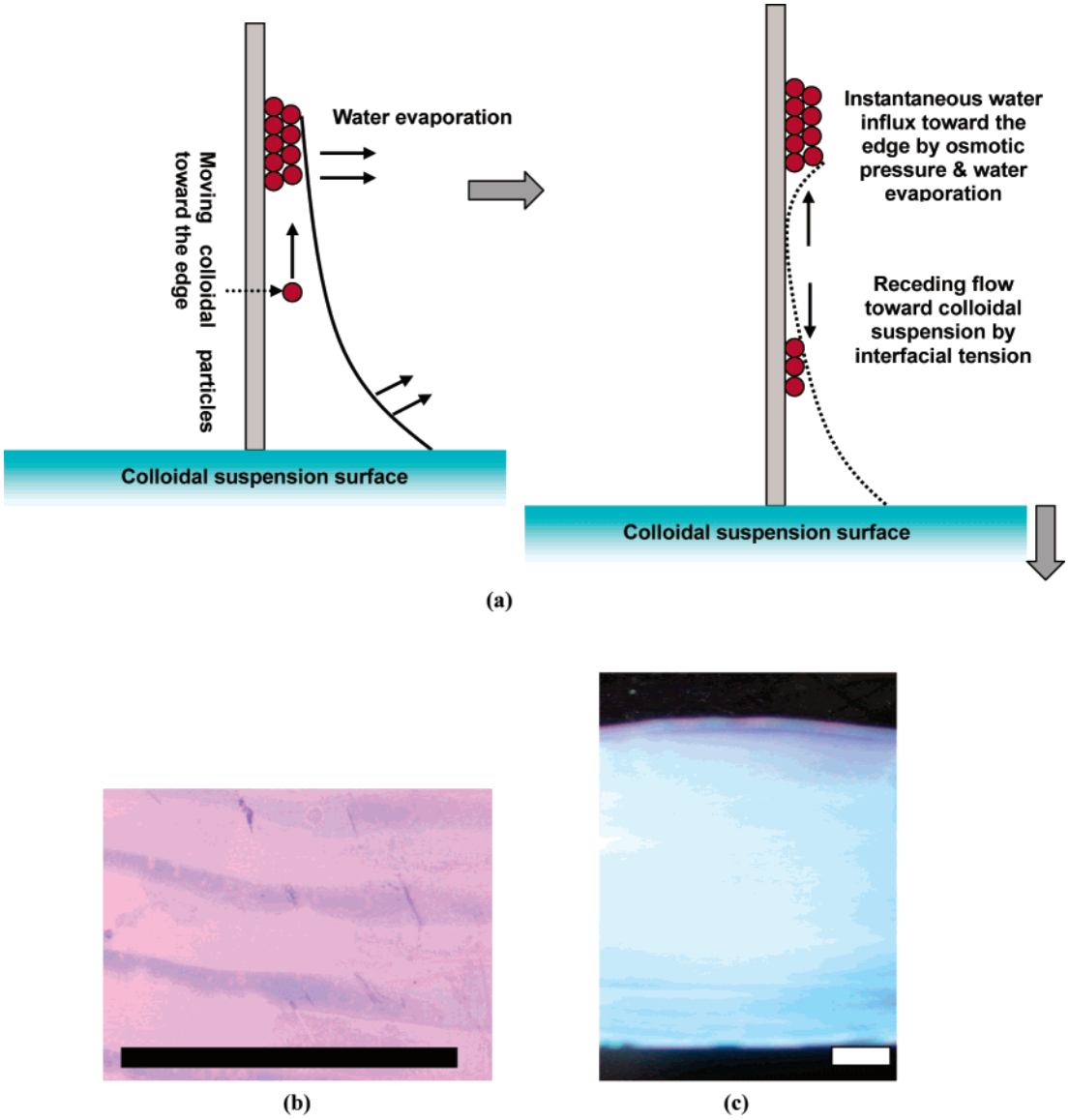

Figure 4. (a) Systematic illustration of the formation of multiple contact line patterns. (b) Optical microscopy image of multiple contact line patterns showing regular interpattern distance (−10° tilted sample). (c) Photograph of 30° tilted sample (tilted incident viewing). No multiple contact line patterns appear. 10° and 20° samples show similar patterns. The scale bars are (b) 1 mm and (c) 5 mm.

colloids show little absorption in the visible region and thus can represent the transmission spectra. We also performed all experiments at 60 °C to minimize defects.[30,45] From the SEM images, as expected with the exception of the sample tilted to 30°, photonic stop band gaps become deeper as the thickness of the colloidal crystals increases. This clearly shows that thicker colloidal crystals show deeper photonic stop band gaps; however, the depth of photonic stop band gaps is saturated above a certain critical thickness of colloidal crystals. The widths of the photonic stop bands decrease as the thickness of the colloidal crystals increase. The observed narrowing of the stop bands with increasing colloidal crystal thickness is reminiscent of the Debye−Scherrer effect in small crystallites.[44] Here, the angular width of a diffraction line is limited by the highest spatial frequency accessible in the reciprocal lattice. The width is thus inversely proportional to the number of lattice planes, and arbitrarily narrow lines should be obtained by increasing the crystal thickness. However, in the colloidal crystals, the narrowing of the stop band with increased colloidal crystals thickness is stopped when colloidal particles are stacked over 10 layers.[44] Therefore, the widths of the stop bands in samples tilted to 20° and 30° are almost the same.

The small and regular peaks around the photonic stop band gaps are Fabry−Perot fringes resulting from interference between reflections from the top and bottom surfaces of the samples while more closely spaced peaks are exhibited in thicker samples.[29]

Deposited Patterns of Colloidal Particles on a Glass Substrate. It is well-established that because the evaporation rate from a pinned drop is greatest at the edge (i.e., the stationary contact line), there is a flow of water toward the edge.[46] This idea was used by Deegan et al.[47,48] to explain why a single ring of micrometer size particles forms on the outside of coffee stains. When the

(45) Im, S. H.; Park, O O. *Langmuir* **2002**, *18*, 9642−9646.

(46) Shmuylovich, L.; Ahen, A. Q.; Stone, H. A. *Langmuir* **2002**, *18*, 3441−3445.

contact line is pinned and evaporation occurs, particles flow toward the contact line and concentrate at the edge. In a similar manner, a colloidal suspension drop on a glass substrate leaves multiple ring stains through pinning and depinning processes.[46] Namely, colloidal particles are pinned and assemble at the air−water−glass substrate interface and form multiple ring patterns via water evaporation. Similar phenomena occur at the air−water−glass substrate interface when a glass substrate is dipped into a colloidal suspension with a tilted angle. Colloidal particles are pinned first at the contact line and move toward the contact line by water influx toward the edge resulting from water evaporation. They then assemble three-dimensionally by capillary force. A systematic illustration is shown in Figure 4a. Once colloidal particles are pinned, the contact line is also pinned. Accordingly, although the level of colloidal suspension by water evaporation becomes lower, the contact line does not move and consequently becomes thinner. When the thickness of the contact line is reduced to that of the colloidal crystals assembled at the contact line edge, the contact line slips by instantaneous water influx toward the edge. (The number of colloidal particles at the edge is much higher and thus the osmotic pressure is also higher. Accordingly, water moves toward the edge to balance concentration.) Similarly, it moves in the direction of water evaporation. (The evaporation rate of water is the highest at the edge.) In addition, the slipped contact line (depinned state) keeps moving until it runs into fixed particles; at which point it may become pinned again.[46] However, we believe that the contact line keeps moving until the interfacial tension becomes stable because the contact line is in an elongated state, and as such it is possible for the pinned contact line to provide the elastic forces.[49] Therefore, the thinned and slipped contact line moves very rapidly to minimize interface energy. The remaining contact line patterns of the −10° tilted sample are shown in Figure 4b. This figure shows that the distance between contact line patterns is constant. This provides important evidence that the slipped contact line is pinned again; at which point the interfacial tension becomes stable. If the slipped contact line were pinned again where it meets fixed particles, the distance between contact line patterns would not be constant.

The conditions for forming multiple contact line patterns are the evaporation rate of water, which is related to the thinning rate of the contact line and instantaneous water evaporation rate, and the contact line shape. (A steeper contact line shape provides easier slip of the pinned contact line.) Accordingly, −10° and 0° tilted samples with relatively steep contact line shapes show multiple contact line patterns (see Figure 1b) and 10°, 20°, and 30° tilted samples do not show multiple contact line patterns (see Figure 4c). The 0° tilted sample prepared at very low evaporation rate (1 mL/day, at 20 °C, 0.2 wt % PS colloidal suspension) does not show any multiple contact line patterns. In addition, the colloidal crystals assembled on the water surface three-dimensionally do not show multiple contact line patterns (see the upper part of Figure 1b shaded in red).

Conclusions

The thickness of colloidal crystals can be controlled by varying the tilted angle of a glass substrate dipped into a colloidal suspension. As the tilted angle increases from −10° to 30°, the contact line shapes become smoother and thus the thickness of formed colloidal crystals increases. When the evaporation rate of water is high, multiple contact line patterns are formed. The conditions involved in the formations of multiple contact line patterns are the evaporation rate of water and the contact line shape. Therefore, to fabricate 3D colloidal crystals with an even surface, it is required to reduce the evaporation rate of water and/or to tilt a glass substrate (any wettable substrate) at an angle greater than 10°.

Acknowledgment. The authors are grateful to the Center for Advanced Functional Polymers, which is supported by KOSEF. This work is also partially supported by the Brain Korea 21 Project.

Supporting Information Available: Representative SEM images (PDF). This material is available free of charge via the Internet at http://pubs.acs.org.

CM021793M

(47) Deegan, R. D.; Bakajin, O.; Dupont, T. F.; Huber, G.; Nagel, S. R.; Witten, T. A. *Nature* **1997**, *389*, 827−829.
(48) Deegan, R. D. *Phys. Rev. E.* **2000**, *61*, 61475−61485.
(49) Decker, E. L.; Garoff, S. *Langmuir* **1997**, *13*, 6321−6322.